

WILEY-VCH

 **Chemistry
Europe**

European Chemical
Societies Publishing

Take Advantage and Publish Open Access



By publishing your paper open access, you'll be making it immediately freely available to anyone everywhere in the world.

That's maximum access and visibility worldwide with the same rigor of peer review you would expect from any high-quality journal.

Submit your paper today.



www.chemistry-europe.org

Charge Transfer

2019 IYPT Is Iron the New Ruthenium?

Oliver S. Wenger*^[a]

Abstract: Ruthenium complexes with polypyridine ligands are very popular choices for applications in photophysics and photochemistry, for example, in lighting, sensing, solar cells, and photoredox catalysis. There is a long-standing interest in replacing ruthenium with iron because ruthenium is rare and expensive, whereas iron is comparatively abundant and cheap. However, it is very difficult to obtain iron complexes with an electronic structure similar to that of ruthenium(II) polypyridines. The latter typically have a long-lived excited state with pronounced charge-transfer character between the ruthenium metal and ligands. These metal-to-ligand charge-transfer (MLCT) excited states can be luminescent, with typical lifetimes in the range of 100 to 1000 ns, and the electrochemical properties are drastically altered during this time. These properties make ruthenium(II) polypyridine complexes so well suited for the abovementioned applications. In iron(II) complexes, the MLCT states


can be deactivated extremely rapidly (ca. 50 fs) by energetically lower lying metal-centered excited states. Luminescence is then no longer emitted, and the MLCT lifetimes become much too short for most applications. Recently, there has been substantial progress on extending the lifetimes of MLCT states in iron(II) complexes, and the first examples of luminescent iron complexes have been reported. Interestingly, these are iron(III) complexes with a completely different electronic structure than that of commonly targeted iron(II) compounds, and this could mark the beginning of a paradigm change in research into photoactive earth-abundant metal complexes. After outlining some of the fundamental challenges, key strategies used so far to enhance the photophysical and photochemical properties of iron complexes are discussed and recent conceptual breakthroughs are highlighted in this invited Concept article.

Commonalities and Differences in the Photo-
physics of Ru^{II} and Fe^{II} Polypyridine Complexes

Most chemical compounds have only very short-lived excited states and do not luminesce after excitation with visible or UV light. Instead, they turn the absorbed energy simply into heat. To obtain luminescent substances with long-lived excited states, a very stringent set of criteria must be fulfilled, and this limits the available chemical space for photophysically and photochemically attractive compounds severely. This is the main reason why certain classes of substances receive much more attention from spectroscopists and photochemists than others. In coordination chemistry, complexes with a metal having a 4d⁶ or 5d⁶ valence electron configuration represent such a privileged class of compounds.^[1] In the vast majority of cases explored to date, this includes precious elements, of which Ru^{II}, Os^{II}, Ir^{III}, and Re^I are the most popular examples. If these metal cations are ligated to organic chelating agents possessing energetically low-lying unoccupied π^* orbitals, then emissive metal-to-ligand charge-transfer (MLCT) excited states with long lifetimes can result.

The [Ru(bpy)₃]²⁺ complex (bpy = 2,2'-bipyridine; Figure 1 a) is the prototype of this substance class, and its simplified electronic structure is illustrated in Figure 1 b and c. An important simplification is that octahedral symmetry is assumed, although the actual symmetry is lower. In the orbital picture in Figure 1 b, the six valence electrons are all paired in three metal-centered (MC) orbitals of t_{2g} symmetry, whereas the e_g orbitals are energetically so high that they remain empty, resulting in a low-spin d⁶-electron configuration. Owing to the strong ligand field in 4d and 5d metals, the t_{2g}-e_g ligand splitting is so large that the π^* orbitals of polypyridine ligands are energetically below the metal e_g orbitals. Consequently, the lowest electronically excited state is of MLCT type, with one of the t_{2g} electrons promoted to the ligand π^* orbital. Notably this is a triplet state because, after initial population of singlet excited states, the heavy metal enables very rapid intersystem crossing.^[2] In the ³MLCT state, the Ru-N distances are only weakly elongated with respect to the ¹A_{1g} electronic ground state, manifesting in ³MLCT and ¹A_{1g} potential wells with small mutual horizontal displacement (Figure 1 c).^[3] The large (vertical) energy gap between the two potentials, combined with

[a] Prof. Dr. O. S. Wenger
Department of Chemistry, University of Basel
St. Johanns-Ring 19, 4056 Basel (Switzerland)
E-mail: oliver.wenger@unibas.ch

 The ORCID identification number(s) for the author(s) of this article can be found under:
<https://doi.org/10.1002/chem.201806148>.

 In celebration of the United Nations International Year of the Periodic Table.

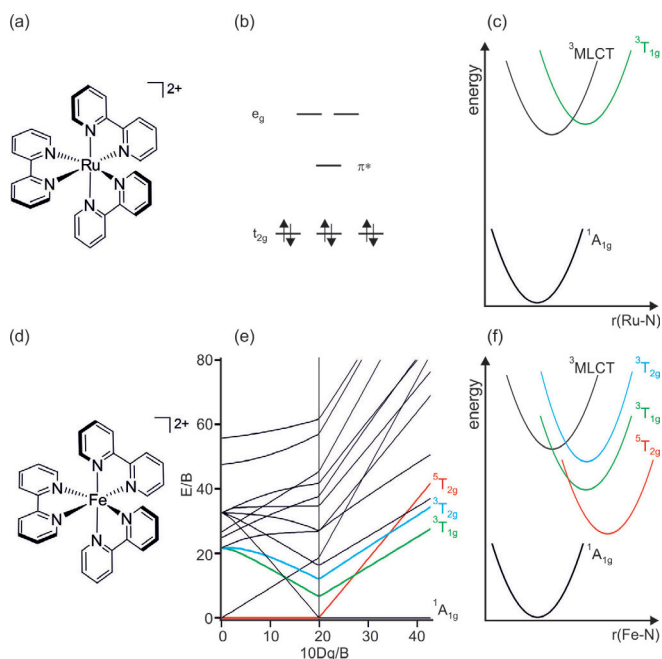


Figure 1. a) Molecular structure of $[\text{Ru}(\text{bpy})_3]^{2+}$; b) the low-spin d^6 electron configuration in O_h symmetry including a low-lying ligand-based π^* orbital in addition to the metal-based t_{2g} and e_g orbitals; c) simplified potential energy diagram with the key electronic states in $[\text{Ru}(\text{bpy})_3]^{2+}$; d) molecular structure of $[\text{Fe}(\text{bpy})_3]^{2+}$; e) Tanabe–Sugano diagram for the d^6 electron configuration; f) simplified potential energy diagram with the key electronic states in $[\text{Fe}(\text{bpy})_3]^{2+}$.

their small mutual displacement along the Ru–N normal coordinate, favors radiative excited-state relaxation. This is in competition with nonradiative deactivation of the ${}^3\text{MLCT}$ state through the MC ${}^3\text{T}_{1g}$ state derived from the excitation of a t_{2g} electron into an e_g orbital. The potential well of that ${}^3\text{MC}$ state (green in Figure 1 c) is markedly displaced along the Ru–N coordinate (typically the a_{1g} normal coordinate) because one electron has moved from a largely nonbonding to an antibonding orbital. This horizontal displacement opens up a pathway for the ${}^3\text{MLCT}$ excited-state population to cross over a certain barrier into the ${}^3\text{T}_{1g}$ state, and from there onwards to the ${}^1\text{A}_{1g}$ ground state.^[4] In $[\text{Ru}(\text{tpy})_2]^{2+}$ (tpy = 2,2':6',2''-terpyridine), the ${}^3\text{T}_{1g}$ state is markedly lower than that in $[\text{Ru}(\text{bpy})_3]^{2+}$, and this is the main reason why $[\text{Ru}(\text{tpy})_2]^{2+}$ is essentially nonemissive at room temperature in fluid solution, whereas $[\text{Ru}(\text{bpy})_3]^{2+}$ has a decent luminescence quantum yield under such conditions.^[5] The lower energy of the ${}^3\text{T}_{1g}$ state in $[\text{Ru}(\text{tpy})_2]^{2+}$ is a direct consequence of the weaker ligand field caused by tpy, relative to bpy, due to smaller N–Ru–N angles.

In Fe^{II} complexes, such as $[\text{Fe}(\text{bpy})_3]^{2+}$ (Figure 1 d), the ligand field is much weaker than that in $[\text{Ru}(\text{tpy})_2]^{2+}$, because the radial distribution of the six 3d electrons is closer to the metal core than that of the 4d electrons in Ru^{II} . Consequently, the ${}^3\text{T}_{1g}$ state and another MC excited state (${}^5\text{T}_{2g}$) are below the ${}^3\text{MLCT}$ state in $[\text{Fe}(\text{bpy})_3]^{2+}$ (Figure 1 f), and three other MC states (${}^3\text{T}_{2g}$, ${}^1\text{T}_{1g}$, ${}^1\text{T}_{2g}$) are energetically close (not all included in Figure 1 f).^[6] In this situation, the ${}^3\text{MLCT}$ state is deactivated within about 50 fs in essentially barrierless fashion, followed

by vibrational cooling on a timescale of a few picoseconds.^[7] The ${}^5\text{T}_{2g}$ state is nonluminescent yet fairly long-lived (ca. 650 ps), which has been exploited in photochemical contexts,^[8] but it would be much more desirable to obtain a long-lived luminescent MLCT state resembling that of $[\text{Ru}(\text{bpy})_3]^{2+}$. To date, this has not yet been achieved with iron.

There are two fairly clear ways to work toward that goal: the ${}^3\text{MLCT}$ state can be energetically stabilized and the MC states should be pushed to higher energies. Lowering of the MLCT state is only viable within the limits of the rules dictated by the energy-gap law,^[9] which basically states that a smaller energy difference between the ${}^3\text{MLCT}$ and ${}^1\text{A}_{1g}$ states results in more efficient direct nonradiative relaxation to the ground state. The effect of an increase in ligand field strength is illustrated by the Tanabe–Sugano diagram for the d^6 -electron configuration (Figure 1 e). The energies of the ${}^3\text{T}_{1g}$ and ${}^5\text{T}_{2g}$ key states rise with increasing ratio between the ligand field strength parameter (Dq) and the Racah parameter (B); the latter is a measure for covalence of the metal–ligand bond. The energy of the ${}^5\text{T}_{2g}$ state (red) is roughly twice as strongly dependent on the ratio of Dq/B as that of the ${}^3\text{T}_{1g}$ state (green) because it involves the excitation of two electrons into antibonding e_g orbitals rather than one, which also manifests in the stronger horizontal displacement of the ${}^5\text{T}_{2g}$ potential well in Figure 1 f. Depending on the ligands, either the ${}^5\text{T}_{2g}$ or ${}^3\text{T}_{1g}$ state is therefore usually the lowest electronically excited state in low-spin Fe^{II} complexes. Increasing the ligand field strength is the key strategy followed by most researchers, and there are various ways to achieve this, as discussed below.

In single configurational coordinate diagrams, such as those in Figure 1 c and f, sometimes harmonic potentials are used for simplicity, although there can be significant degrees of anharmonicity. Usually identical force constants are assumed for the electronic ground state and different types of excited states, and this represents a further simplification. The normal coordinate on the x axis often represents an essentially totally symmetrical (a_{1g}) distortion, but the types of relevant nuclear coordinates can be different from one compound to another.^[10]

Each of the following six sections discusses one of six key concepts to achieve long-lived MLCT excited states in Fe^{II} complexes. This includes the creation of highly symmetric ligand fields (Figure 2 a), the use of push–pull ligand sets (Figure 2 b), highly strained complexes giving access to ${}^5\text{MLCT}$ states (Figure 2 c), exploitation of strong σ donation provided by N-heterocyclic carbene (NHC) ligands (Figure 2 d), combined σ and π donation by cyclometalating ligands (Figure 2 e), and the use of mesoionic carbenes as combined σ donor, π acceptor ligands (Figure 2 f). Subsequently, the recent conceptual breakthrough leading to emissive Fe^{III} complexes is highlighted, and some alternatives based on other earth-abundant metal elements are discussed very briefly.

Concept I: High Symmetry

One way to enhance the ligand field is to design chelating agents that permit coordination of Fe^{II} with bond angles as close as possible to those of the ideal octahedral coordination

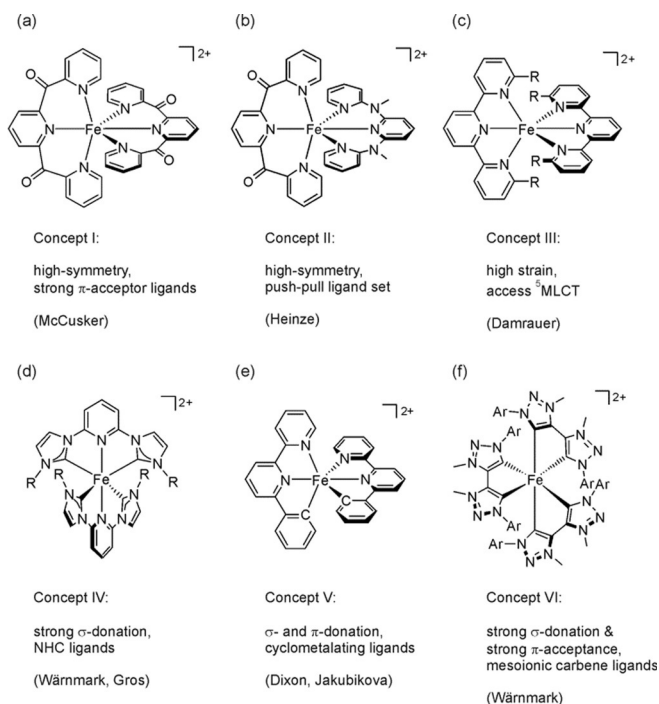


Figure 2. Key strategies and concepts for obtaining Fe^{II} complexes with long-lived MLCT states, along with exemplary molecular structures: a) $[\text{Fe}(\text{dcpp})_2]^{2+}$ (dcpp = 2,6-bis(2-carboxypyridyl)pyridine,^[11] b) $[\text{Fe}(\text{dcpp})(\text{ddpd})]^{2+}$ (ddpd = *N,N'*-dimethyl-*N,N'*-dipyridine-2-yl-pyridine-2,6-diamine),^[12] c) $[\text{Fe}(\text{dftpy})_2]^{2+}$ (6,6'-difluoro-2,2':6',2''-terpyridine; R = F), $[\text{Fe}(\text{dctpy})_2]^{2+}$ (dctpy = 6,6'-dichloro-2,2':6',2''-terpyridine; R = Cl), $[\text{Fe}(\text{dbtpty})_2]^{2+}$ (dbtpty = 6,6'-bromo-2,2':6',2''-terpyridine; R = Br),^[13] d) $[\text{Fe}(\text{C}_{\text{NHC}}-\text{N}_{\text{pyridine}}-\text{C}_{\text{NHC}})]_2^{2+}$ with R = CH₃,^[14] R = *t*Bu,^[15] and R = *i*Pr,^[16] e) bis(terdentate) complexes with cyclometalating 2,2':6',2''-terpyridine (tpy)-derived ligands,^[17] f) $[\text{Fe}(\text{btz})_3]^{2+}$ (btz = 4,4'-bis(1,2,3-triazol-5-ylidene); Ar = *p*-C₆H₄-Me).^[18]

geometry, that is, 180° for N-Fe-N *trans* angles. This maximizes overlap between the metal and ligand orbitals contributing to the coordination bond. McCusker and co-workers used a tridentate ligand with three pyridine binding motifs linked through carbonyl groups, resulting in N-Fe-N *trans* angles of 178.3° in the $[\text{Fe}(\text{dcpp})_2]^{2+}$ complex (Figure 2a).^[11] For reference, in $[\text{Ru}(\text{tpy})_2]^{2+}$ the N-Ru-N *trans* angles are 158.6°,^[5] hence the bite angle adoptable for dcpp is much more favorable. Perhaps even more significant is the electron-withdrawing nature of the carbonyl groups, which leads to an energetic stabilization of the lowest π^* orbital of the dcpp ligand. This leads to better energetic match with the filled t_{2g} orbitals of the Fe^{II} center, which, in turn, causes increased metal-ligand orbital mixing and stabilization of the t_{2g} orbitals (Figure 3c), that is, dcpp is a strong π acceptor ligand. Thus, the ligand field in $[\text{Fe}(\text{dcpp})_2]^{2+}$ is roughly 600 meV stronger than that in $[\text{Fe}(\text{tpy})_2]^{2+}$, manifesting in an unusual blue color (purple is more typical for Fe^{II} polypyridines) and a substantially higher electrochemical potential for (metal-based) one-electron oxidation. In acetonitrile at room temperature, $[\text{Fe}(\text{dcpp})_2]^{2+}$ has an excited state with a lifetime of 280 ps, and it is not a priori clear what type of ligand-field state this is. In $[\text{Fe}(\text{tpy})_2]^{2+}$, $^5\text{T}_{2g}$ is the lowest excited state, which decays with a lifetime of 960 ps under identical conditions.^[11] Possibly, the ligand field in

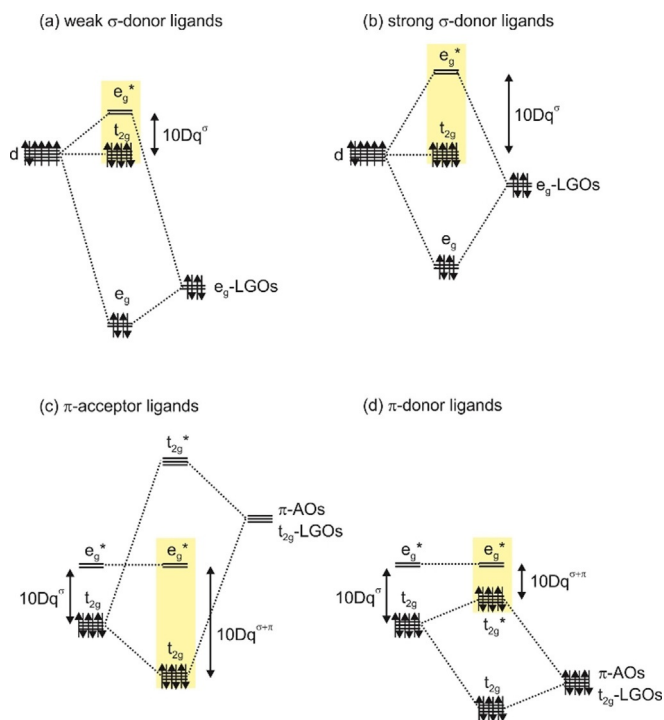


Figure 3. Ligand field effects depending on the type of bonding interactions between metal d orbitals and ligand group orbitals (LGOs) or atomic orbitals (AOs). The vertical axes are energy axes. The key point is the magnitude of the ligand field strength ($10Dq$), which is given as the energy difference between t_{2g} and e_g orbitals (marked in yellow).

$[\text{Fe}(\text{dcpp})_2]^{2+}$ is so strong that $^3\text{T}_{1g}$ instead of $^5\text{T}_{2g}$ is lowest (green vs. red in Figure 1e), and this could be the origin of the faster excited-state decay, for two key reasons: 1) the electronic coupling between $^3\text{T}_{1g}$ and $^1\text{A}_{1g}$ is likely to be stronger than that between $^5\text{T}_{2g}$ and $^1\text{A}_{1g}$ because of the smaller change of net spin, and 2) the reorganization energy associated with the transition from $^3\text{T}_{1g}$ to $^1\text{A}_{1g}$ is smaller because it involves the relaxation of a single e_g electron to a t_{2g} orbital, whereas the transition from $^5\text{T}_{2g}$ to $^1\text{A}_{1g}$ involves the relaxation of two electrons from antibonding e_g to formally nonbonding t_{2g} orbitals. Both of these effects are expected to make relaxation from the $^3\text{T}_{1g}$ faster than that from the $^5\text{T}_{2g}$; this is in line with the observation that the excited state of $[\text{Fe}(\text{dcpp})_2]^{2+}$ decays more rapidly than that of the $^5\text{T}_{2g}$ state of $[\text{Fe}(\text{tpy})_2]^{2+}$ (280 vs. 960 ps).

The $[\text{Fe}(\text{dcpp})_2]^{2+}$ study by McCusker and co-workers very nicely illustrates the concepts of coordination geometry optimization and ligand π^* -acceptor property tuning. Computational work by Jakubikova and co-workers supports the interpretation of these experimental results, and further suggests that replacement of the central pyridine unit of the dcpp ligand with a five-membered NHC or cyclometalating phenyl unit would provide an even stronger ligand field.^[19]

Concept II: Push-Pull Systems with High Symmetry

Heinze and co-workers combined the electron-withdrawing dcpp chelate of McCusker with the electron-rich ddpd ligand

to obtain the heteroleptic $[\text{Fe}(\text{dcpp})(\text{ddpd})]^{2+}$ complex (Figure 2b).^[12] Similar to dcpp, the ddpd ligand is able to chelate Fe^{II} in a terdentate fashion with favorable N-Fe-N angles, but it is much more electron rich because there are amine instead of carbonyl groups in the backbone.^[20] The aim was to exploit the resulting push-pull ligand combination to lower the $^1/3\text{MLCT}$ manifold of Fe^{II} complexes, while, at the same time, raising the $^3\text{T}_{1g}$ and $^5\text{T}_{2g}$ states through increased metal-ligand orbital overlap facilitated by the favorable bite angles of these two particular ligands. $[\text{Fe}(\text{dcpp})(\text{ddpd})]^{2+}$ exhibits low-lying absorption bands with maxima at $\lambda = 585$ and 559 nm of mixed MLCT and ligand-to-ligand charge-transfer (LLCT) character (ddpd \rightarrow dcpp). However, following excitation at $\lambda = 500$ nm, picosecond transient absorption spectroscopy fails to provide any evidence for excited-state absorptions that would be clearly attributable to MLCT or LLCT states. Instead, it was concluded that internal conversion to a MC state occurred. The observable ground-state recovery, with a time constant of 548 ps, was tentatively attributed to the $^3\text{T}_{1g}$ state,^[12] following the interpretation by McCusker and co-workers that dcpp induces a ligand field strength approaching the $^5\text{T}_{2g}/^3\text{T}_{1g}$ crossing point (Figure 1 e), or possibly even exceeding it.^[11] The approach of obtaining luminescent LLCT (instead of MLCT) states in push-pull complexes with Fe^{II} seems very promising with a variant of ddpd in which the amines are not methylated, but merely bear a hydrogen atom.^[21]

Concept III: Accessing $^5\text{MLCT}$ States in Strained Low-Spin Complexes

Damrauer and co-workers explored a fundamentally different concept in homoleptic Fe^{II} complexes with tpy ligands that were halogenated at the 6- and 6'-positions (Figure 2c).^[13] The ligand field in the chloro- and bromo-substituted $[\text{Fe}(\text{dctpy})_2]^{2+}$ and $[\text{Fe}(\text{dbtpy})_2]^{2+}$ complexes is substantially weaker than that in the $[\text{Fe}(\text{tpy})_2]^{2+}$ parent compound, due to repulsive interactions between the halogen atoms from one tpy ligand to the second (opposing) tpy. Consequently, $^5\text{T}_{2g}$ rather than $^1\text{A}_{1g}$ is the electronic ground state, as expected for weak-field ligands (Figure 1 e). In the fluoro-substituted $[\text{Fe}(\text{dftpy})_2]^{2+}$ complex, $^5\text{T}_{2g}$ and $^1\text{A}_{1g}$ are populated in a ratio of 97%:3% at room temperature. Thus, it is possible to excite each of the three complexes into a spin-allowed $^5\text{T}_{2g} \rightarrow ^5\text{MLCT}$ transition, and subsequent decay of the $^5\text{MLCT}$ state (or $^7\text{MLCT}$ in the event of intersystem crossing) can be monitored. This is fundamentally different from the $^3\text{MLCT}$ states, which are typically populated through intersystem crossing after $^1\text{A}_{1g} \rightarrow ^1\text{MLCT}$ excitation of low-spin Fe^{II} complexes. The key finding is that the $^5/7\text{MLCT}$ lifetime increases from 14.0 ps to 16.0 and 17.4 ps along the F, Cl, and Br series of complexes (in acetonitrile at room temperature).^[13a] Direct nonradiative passage between the $^5/7\text{MLCT}$ and $^5\text{T}_{2g}$ states seems unlikely, and a decay path involving $^3\text{T}_{1g}$ (or other nearby ^3MC states) is more plausible. The energy of the relevant ^3MC state should be fairly sensitive to size of the halogen substituent because this state derives from an electron configuration with greater net metal-ligand bonding character than the $^5/7\text{MLCT}$ and $^5\text{T}_{2g}$ states. The observation of slower

$^5/7\text{MLCT}$ decay with larger halogen size is compatible with an increasing barrier to interconversion from $^5/7\text{MLCT}$ to ^3MC , which is caused by a shift of the ^3MC potential well to higher energies, closer to the $^5/7\text{MLCT}$ potential well (red circle in Figure 4). Moreover, a larger halogen atom means it is more

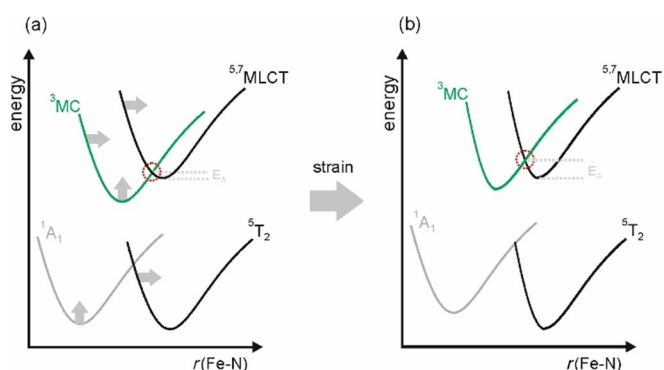


Figure 4. Illustration of the effects of increasing steric hindrance along the series $[\text{Fe}(\text{dftpy})_2]^{2+}$, $[\text{Fe}(\text{dctpy})_2]^{2+}$, and $[\text{Fe}(\text{dbtpy})_2]^{2+}$ ($\text{R} = \text{F}, \text{Cl}$, and Br in Figure 2c) on the relevant potential-energy surfaces.^[13] a) Comparatively little strain ($\text{R} = \text{F}$); b) comparatively strong strain ($\text{R} = \text{Br}$). The activation energy (E_a) for crossing from $^5\text{MLCT}$ to ^3MC increases from a) to b). Gray arrows in a) mark the effects of increasing strain coming into effect in b).

difficult energetically for the $^5/7\text{MLCT}$ state to adopt geometries needed for conversion to the ^3MC state. In other words, halogen exchange along the series F, Cl, and Br leads to an increase of the reorganization energy for internal conversion, and this could contribute to lengthening of the $^5/7\text{MLCT}$ lifetime. The key concept pursued in this work can be described as the exploitation of interligand steric interactions to control relative state energies and to limit conformational dynamics.^[13] The increase of the $^5/7\text{MLCT}$ lifetime along the F, Cl, and Br series of Fe^{II} complexes is somewhat reminiscent of the counter heavy-atom effect observed for intersystem crossing rates in Re^{I} complexes.^[22]

Concept IV: Enhancement of Ligand Field Strength with σ -Donating NHC Ligands

In the McCusker $[\text{Fe}(\text{dcpp})_2]^{2+}$ complex (Figure 2a), the pronounced π -acceptor properties of the dcpp ligand cause a strong ligand field by stabilizing the t_{2g} orbitals (see above). A complementary strategy to increasing the ligand field strength is to destabilize the e_g orbitals with strongly σ -donating ligands (Figure 3 a and b). This is the key concept behind the use of NHC ligands for Fe^{II} complexes (Figure 2d), as first investigated in the context of obtaining long-lived $^3\text{MLCT}$ excited states by Wärnmark and co-workers.^[14] This very promising area has been reviewed,^[23] and several different research groups have made important recent contributions.

In a pioneering study, a $^3\text{MLCT}$ lifetime of 9 ps (in CH_3CN at room temperature) was reported for a homoleptic complex with the terdentate 2,6-bis(imidazol-2-ylidene)pyridine ligand (Figure 2d), and this was the longest known $^3\text{MLCT}$ lifetime for Fe^{II} complexes at the time (2013).^[14] The $\text{C}_{\text{NHC}}\text{-N}_{\text{pyridine}}\text{-C}_{\text{NHC}}$

ligand design cleverly exploits the fact that NHCs are strong σ donors (Figure 3b), but, at the same time, takes into consideration that their π -acceptor properties are limited. For this reason, the pyridine unit is integrated to accommodate the MLCT-excited electron. Unfortunately, the $^3\text{MLCT}$ energy is nevertheless raised relative to $[\text{Fe}(\text{tpy})_2]^{2+}$ due to modest π -acceptor abilities, and this can be counteracted, to some extent, by increasing π conjugation upon replacing imidazolylidene with benzimidazolylidene subunits (Figure 5a), yielding a

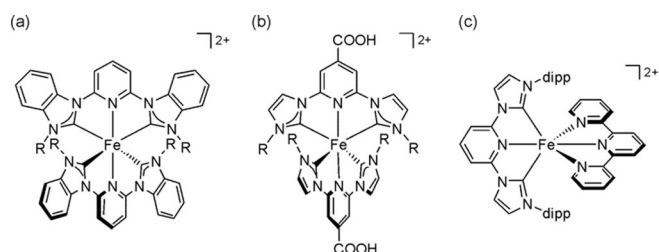


Figure 5. Molecular structures of Fe^{II} complexes with NHC ligands: a) benzimidazolylidene-based analogue of the complex in Figure 2d ($\text{R}=\text{CH}_3$);^[24] b) carboxyl-substituted analogue of the prototype complex in Figure 2d ($\text{R}=\text{CH}_3$);^[24-25] c) heteroleptic Fe^{II} NHC-tpy complex (dipp = diisopropylphenyl).^[16]

$^3\text{MLCT}$ lifetime of 16 ps, as reported by Gros and co-workers,^[24] or by attaching carboxyl groups to the pyridine unit. Relative to the parent complex in Figure 2d ($\text{R}=\text{CH}_3$), the carboxyl-functionalized complex in Figure 5b ($\text{R}=\text{CH}_3$) has its MLCT absorption maximum redshifted by about 2000 cm^{-1} , and its $^3\text{MLCT}$ lifetime is lengthened from 9 to 16–18 ps in acetonitrile,^[25] or 37 ps on Al_2O_3 nanofilm.^[25b] Upon attachment to TiO_2 , this photoexcited complex injects electrons into the conduction band with a time constant of 3.1 ps and a 92% conversion of photons to electrons, but unfortunately only 13% of the resulting charge-separated states persist on the nanosecond timescale.^[25b] This could be a reason for the modest performance of a dye-sensitized solar cell device with this particular sensitizer reported by Gros and co-workers.^[25a] Subsequent studies by the same group, including a heteroleptic Fe^{II} -NHC complex provided similar results with regard to photovoltaic efficiency in sensitized solar cells.^[26] However, computational work by Persson and co-workers found that Fe^{II} complexes with $\text{C}_{\text{NHC}}\text{-N}_{\text{pyridine}}\text{-C}_{\text{NHC}}$ ligands had intrinsic electronic properties that were well suited to promote charge separation through very rapid ($\approx 100\text{ fs}$) electron injection into the conduction band of TiO_2 .^[27] A computational perspective of Fe^{II} polypyridines as dyes in solar cells has been published recently by Jakubikova and Bowman.^[28]

An alternative strategy to keep the $^3\text{MLCT}$ energy low, while still exploiting strong σ donation provided by NHC ligands, is the synthesis of heteroleptic complexes, in which a $\text{C}_{\text{NHC}}\text{-N}_{\text{pyridine}}\text{-C}_{\text{NHC}}$ chelator is combined with a traditional polypyridine ligand, such as tpy.^[29] A complex of this type (Figure 5c) has been used by Bauer and co-workers for photosensitization of water reduction.^[30] The bulky dipp substituents used in this case prevent the formation of homoleptic $\text{C}_{\text{NHC}}\text{-N}_{\text{pyridine}}\text{-C}_{\text{NHC}}$ complexes.

The N-substituents themselves have an important influence on the ligand field strength and achievable $^3\text{MLCT}$ lifetime, particularly in homoleptic complexes with the basic structure shown in Figure 2d. According to X-ray crystallographic studies, the Fe–C bonds are 0.13 Å shorter in the complex with $\text{R}=\text{CH}_3$ than those for $\text{R}=\text{tBu}$ because of steric repulsion between the tBu groups of one ligand with the pyridine moiety of the other.^[14] Consequently, the ligand field in the complex with $\text{R}=\text{tBu}$ is weaker and the $^3\text{MLCT}$ lifetime is considerably shorter ($\approx 0.3\text{ ps}$ for $\text{R}=\text{tBu}$ compared with 9 ps for $\text{R}=\text{CH}_3$). For $\text{R}=\text{iPr}$, a $^3\text{MLCT}$ lifetime of 8.1 ps was found;^[16] hence there is some correlation between the size of R and the $^3\text{MLCT}$ lifetime. Bauer and co-workers further established a correlation between NHC donor count and the photophysical properties of Fe^{II} complexes.^[16] The sterically most congested complex ($\text{R}=\text{tBu}$ in Figure 2d), exhibiting the shortest $^3\text{MLCT}$ lifetime ($\approx 0.3\text{ ps}$), was recently explored by means of time-resolved X-ray scattering in combination with DFT.^[15] After MLCT excitation of this complex, its $^5\text{T}_2$ state, at an energy of 0.75 eV, is rapidly populated and then decays to the ground state with a lifetime of 260 ps. The key finding is that the metal–ligand bonds are very strongly elongated in this $^5\text{T}_2$ state. Compared with the $^1\text{A}_1$ ground state, the axial Fe–N bonds are longer by 0.29 Å, whereas the equatorial Fe–C distances increase by 0.21 Å.^[15] For a structurally related complex with $\text{R}=\text{CH}_3$ (Figure 2d), even more significant elongations of 0.34 (for axial Fe–N bonds) and 0.25 Å (for equatorial Fe–C bonds) were calculated for the $^5\text{T}_2$ state.^[15,31] In this case, the $^3\text{MLCT}$ lifetime is 9 ps, as noted above, and there is no experimental evidence for population of the highly distorted $^5\text{T}_{2g}$ in the course of $^3\text{MLCT}$ deactivation. This contrasts the frequently invoked $^3\text{MLCT}\rightarrow^3\text{MC}\rightarrow^5\text{MC}$ or $^3\text{MLCT}\rightarrow^5\text{MC}$ relaxation pathways for $[\text{Fe}(\text{bpy})_3]^{2+}$ and $[\text{Fe}(\text{tpy})_2]^{2+}$ (Figure 6a), and is due to the unusually large structural distortions required to access the ^5MC state in the carbene complexes. Instead, calculations combined with experiments clearly indicate a $^3\text{MLCT}\rightarrow^3\text{MC}$ relaxation, followed by direct deactivation of the latter into the ground state (Figure 6b), bypassing the ^5MC state.^[14,31]

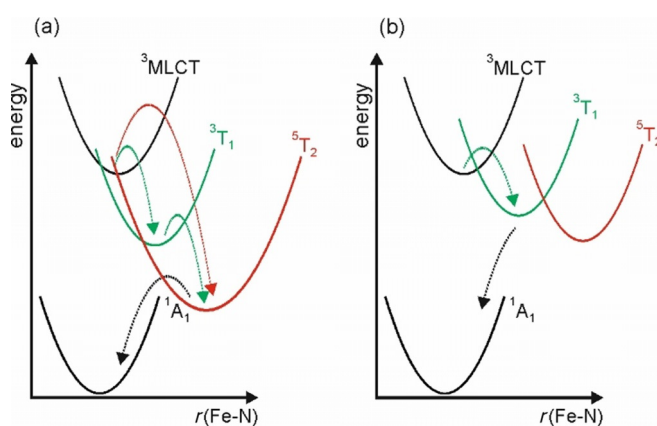


Figure 6. Simplified schematic representations of $^3\text{MLCT}$ relaxation pathways in classic Fe^{II} polypyridine complexes, such as $[\text{Fe}(\text{bpy})_3]^{2+}$ and $[\text{Fe}(\text{tpy})_2]^{2+}$ (a),^[7a,b] and in Fe^{II} NHC complexes (b).^[14,31]

Recent computational work by Monari and co-workers demonstrated that there could be subtle but important differences in the ³MLCT deactivation pathways for *fac* and *mer* isomers of the same Fe^{II}-carbene complex, and they concluded that Fe–N bond elongation was the key normal coordinate leading to triplet relaxation.^[32] Their work underscores the importance of complete calculation of the potential-energy surfaces to adequately describe excited-state relaxation.

The finding that the ⁵MC state does not seem to be involved in the ³MLCT deactivation of Fe^{II}-NHC complexes is an important conceptual difference from that of traditional Fe^{II} polypyridine complexes (Figure 6). It illustrates that, if an undesired MC state is sufficiently strongly distorted, then it may not play a significant role, even if it lies at relatively low energy.

Concept V: Stabilization of MLCT States/Destabilization of MC States with Cyclometalating σ - and π -Donor Ligands

The idea of using cyclometalating chelate ligands to obtain photoactive Fe^{II} complexes (Figure 2e) has been promoted by the computational groups of Dixon and Jakubikova, whereas experimental investigations seem to be less far advanced, to date. However, some intriguing predictions have emerged from DFT and time-dependent (TD) DFT calculations, mostly concerning bis(tridentate) complexes with variable numbers and positions of cyclometalating phenyl units. Upon replacing tpy with structurally related N[^]N[^]^C or N[^]^C[^]N ligands, such as those shown in Figures 2e and 7a, MLCT states are strongly

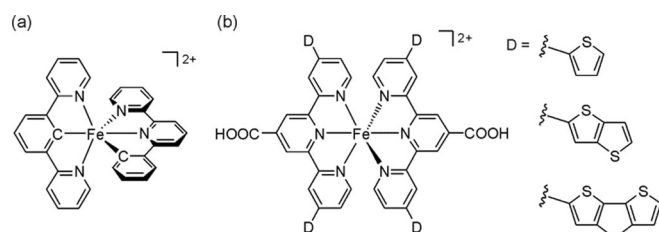


Figure 7. Examples of candidate complexes predicted to be interesting by calculations: a) $[\text{Fe}(\text{N}^{\wedge}\text{C}^{\wedge}\text{N})(\text{N}^{\wedge}\text{N}^{\wedge}\text{C})]^{2+}$,^[17a,b] b) complexes with π -donating ligands, some of them leading to “HOMO inversion”.^[35]

stabilized (ca. 1 eV) due to the pronounced π -donating character of the cyclometalating ligands (Figure 3d),^[17b] leading to a redshift of the respective absorption bands.^[17c] The ³MC states are less influenced by cyclometalation (ca. 0.2 eV), which implies that the destabilization of the e_g orbitals by σ donation (Figure 3b) is of similar magnitude to that of destabilization of the t_{2g} orbitals by π donation (Figure 3d).^[17b] However, the photophysically most relevant ³MC state is destabilized only if the ligating C atoms are on one of the peripheral rings of the tridentate ligand; instead, if they are on the central ring, an undesirable stabilization of ³MC results.^[17b,33] The complexes shown in Figure 2e and 7a were therefore identified as particularly promising with regard to avoiding population of the ³MC state out of the ³MLCT state.^[17b,c] Cyclometalation increas-

es the energy difference between the ¹A₁ and ⁵T states by 8–19 kcal mol⁻¹; the exact amount depends on the number and position (center or side) of the aryl groups.^[17a] Overall, these calculations all predict that cyclometalation has the potential to slow relaxation from the ^{1/3}MLCT states into the ³MC and ⁵MC states.^[17] On the other hand, experimental work by Heinze and co-workers found that cyclometalating ligands led to Ru^{II} complexes that were less useful than anticipated, exhibiting only very weak photoluminescence in solution at room temperature.^[34]

Dixon and co-workers noted that only up to two pyridine ligands could be replaced by phenyl units; otherwise the iron center would no longer be in the +II oxidation state.^[17c] This is an interesting aspect, in view of the very recent discovery of photoluminescence from two Fe^{III} complexes (see below). A recent DFT study by Jakubikova and co-workers addressed the issue of oxidative stability of cyclometalated Fe^{II} complexes.^[36]

Complementary work aimed to computationally identify ligands that might provide Fe^{II} complexes, in which ³MLCT states are energetically lower than the ³MC states. In addition to NHC-type (chelate) ligands, strongly σ -donating acetylide-based systems seemed to be particularly promising.^[37]

Recently, Jakubikova and co-workers reported on a computational study focused on improving the optical absorption properties of Fe^{II} polypyridines; this work provided particularly interesting insights regarding the importance of the π -donation properties of the ligands.^[35] The tpy ligands substituted with furan, thiophene, and selenophenes (Figure 7b) were found to have occupied π orbitals that were energetically better aligned with the t_{2g} orbitals on Fe^{II}; thus leading to stronger metal–ligand π interactions and a consequent increase of the HOMO energy (Figure 3d). This results in multiple mixed MLCT/ILCT (ILCT=intraligand charge transfer) transitions in the calculated absorption spectrum. If donor groups with more extended π conjugation were attached to tpy (e.g., thienothiophene, dithienothiophene), further stabilization of the ligand π orbitals resulted in a ligand-centered HOMO; this effect has been termed HOMO inversion.^[35] This is conceptually very interesting, but at this point it is unclear how relaxation of the resulting low-lying LLCT excited states will take place, in particular, how competitive radiative processes will be.

Experimental work by Dietzek and co-workers demonstrated that the use of tpy ligands with extended π -conjugated groups in the 4'-position could represent a viable strategy to obtain relatively long-lived ³MLCT states in $[\text{Fe}(\text{tpy})_2]^{2+}$ compounds.^[38] In a molecular triad comprised of a central $[\text{Fe}(\text{tpy})_2]^{2+}$ unit flanked by two peripheral $[\text{Ru}(\text{tpy})_2]^{2+}$ chromophores through *p*-phenylene vinylene linkers, a ³MLCT lifetime of 26 ps was measured for the central Fe^{II} unit.^[38]

Concept VI: Combined Strong σ -Donation and π -Acceptance with Mesoionic Carbene Ligands

NHC ligands are strong σ donors, but relatively weak π acceptors (Concept IV). Wärnmark, Sundström and co-workers found that the mesoionic carbene ligand btz (Figures 2f and 8) acted as both a stronger σ donor and π acceptor than classic

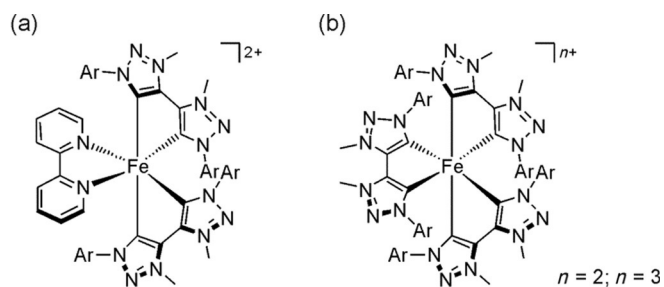


Figure 8. Fe^{II} and Fe^{III} complexes with mesoionic carbene ligands: a) [Fe(btaz)₂(bpy)]²⁺;^[39] b) [Fe(btaz)₃]²⁺ (*n* = 2);^[18] [Fe(btaz)₃]³⁺ (*n* = 3);^[41] Ar = *p*-C₆H₄-Me.

NHCs.^[39] The uncommon {Fe(bpy)Cl₂} intermediate gave access to the heteroleptic [Fe(btaz)₂(bpy)]²⁺ complex (Figure 8a) with a ³MLCT lifetime of 13 ps, which was 100 times longer than that in [Fe(bpy)₃]²⁺. The new complex is photochemically robust, even during overnight laser experiments.^[39] Compared with normal NHC ligands, btz has a formal negative charge on the carbene C atom in one resonance structure;^[40] on this basis, it becomes readily understandable why btz is a stronger σ donor. At the same time, the increased number of N atoms lowers its π^* energy relative to normal NHC ligands, which makes it a stronger π acceptor (Figure 3c).^[39] In the very strong ligand field imposed by btz, the ³MC and ⁵MC states are destabilized and their minima displaced far away from that of the ³MLCT state; thus making undesired nonradiative relaxation comparatively inefficient.

In the homoleptic [Fe(btaz)₃]²⁺ complex (Figures 2f and 8b; *n* = 2), these effects are even more dramatic. Biexponential transient absorption kinetics with time constants of 3.6 and 528 ps were observed, and the 3.6 ps dynamics were attributed to initial vibrational cooling or excited-state electronic transitions into lower-lying excited states.^[18] The 528 ps dynamics are fully compatible with ³MLCT decay, showing the excited-state absorption features typically associated with an MLCT state. Given this record lifetime, some near-infrared photoluminescence could be anticipated, but this remained undetectable at a threshold of about 10⁻⁴ for the luminescence quantum yield. However, in that ³MLCT state, about 1.0 eV above the ground state, [Fe(btaz)₃]²⁺ is a strong photoreductant with an oxidation potential of -1.6 V versus the ferrocenium/ferrocene (Fc^{+/0}) couple.^[18] For reference, the oxidation potential of ³MLCT-excited [Ru(bpy)₃]²⁺ is -1.2 V versus the same reference electrode;^[42] hence [Fe(btaz)₃]²⁺ would be readily useable as a photoredox catalyst.

Concept VII: Fe^{III} instead of Fe^{II}, Spin-Allowed LMCT instead of Spin-Forbidden MLCT

When reacting btzH⁺ with an Fe^{II} source (FeBr₂) and base (*t*BuOK) in THF followed by aqueous workup, one obtains the [Fe(btaz)₃]³⁺ complex, not the [Fe(btaz)₃]²⁺ compound discussed in the previous section.^[41] The latter is then amenable by reduction of the Fe^{III} complex with dithionite.^[18] However, the photophysical properties of the Fe^{III} complex are even more

spectacular than those of the Fe^{II} compound. [Fe(btaz)₃]³⁺ (Figure 8b, *n* = 3) has a low-spin 3d⁵ electron configuration, according to Mössbauer spectroscopy, X-ray absorption, and quantum chemical calculations,^[41,43] resulting in a ²T₂ ground state (Figure 9a). This complex exhibits LMCT absorptions with band maxima at λ = 528 and 558 nm, in agreement with the metal reduction and ligand oxidation potentials determined by electrochemical methods. Excitation into these absorption bands leads to visible ²LMCT emission with a quantum yield of 3 × 10⁻⁴ in CH₃CN at room temperature.^[41] Thus, an Fe^{III}, not an Fe^{II}, species has quite unexpectedly become the first iron complex exhibiting photoluminescence from a charge-transfer state.^[44]

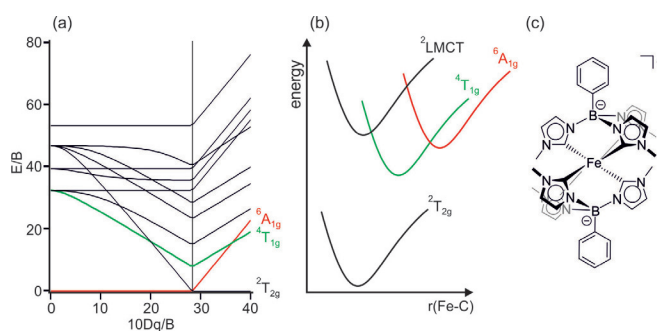


Figure 9. a) Tanabe-Sugano diagram for the d⁵-electron configuration; b) simplified schematic potential-energy diagram involving key electronic states in [Fe(btaz)₃]³⁺;^[41] c) molecular structure of [Fe(phtmeimb)₃]⁺ (phtmeimb = {phenyl[tris(3-methylimidazol-1-ylidene)]borate})^[45]

The ²LMCT state decays to the ground state with a lifetime of 100 ps without observable population of MC states. Upon comparing the relevant parts of the Tanabe-Sugano diagrams for d⁵- (Figure 9a) and d⁶-electron configurations (Figure 1e), one readily recognizes some similarities with respect to MC states in the respective strong-field limits. In both cases, there are low-lying MC states accessible by either two- (⁵T₂ for d⁶, ⁶A₁ for d⁵) or one-electron excitation (³T₁ for d⁶, ⁴T₁ for d⁵). **Accordingly, the ⁶MC and ⁴MC potentials have their minima at substantially extended Fe-C bond coordinates (Figure 9b), similar to the ⁵MC and ³MC states in Fe^{II} complexes (Figure 6b).** Calculations further indicate that the ⁶MC and ⁴MC potential minima are at relatively high energy due to the strongly σ -donating character of btz. Moreover, the Stokes shift between ²LMCT absorption and emission amounts to only 0.15 eV, which indicates that the ²LMCT state is only weakly distorted relative to the ground state. Thus, similar to the lowest ³MLCT states in many of the Fe^{II} complexes discussed above, there are sizeable barriers for the deactivation of the emissive ²LMCT state via MC states (Figure 9b). Based on temperature-dependent lifetime measurements, an Arrhenius model with two exponential functions yielded activation barriers of 4 and 22 kJ mol⁻¹.^[41]

Aside from the direction of optical charge transfer, there is yet another major difference to Fe^{II} complexes. The MLCT states of key interest in the latter are spin triplets, and radiative rate constants for luminescence to the singlet ground state are

expected to be relatively small because of the spin-forbidden (phosphorescence-type) nature of the process. By contrast, emission from the ${}^2\text{LMCT}$ state to the ${}^2\text{T}_2$ ground state in $[\text{Fe}(\text{btz})_3]^{3+}$ is a spin-allowed (fluorescence-type) process; thus making radiative relaxation inherently more competitive with nonradiative deactivation. Specifically, a radiative rate constant of $3 \times 10^6 \text{ s}^{-1}$ was determined for the ${}^2\text{LMCT} \rightarrow {}^2\text{T}_2$ transition in $[\text{Fe}(\text{btz})_3]^{3+}$.

These highly interesting findings were recently topped by a study of the same Swedish–Danish consortium, reporting on room-temperature photoluminescence from a ${}^2\text{LMCT}$ state with a lifetime of 2.2 ns and a quantum yield of 2%.^[45] This is a truly amazing result, and it motivated the title of this Concept article. The $[\text{Fe}(\text{phtmeimb})_2]^+$ complex (Figure 9c) has two anionic scorpionate-like tris(carbene) ligands, which were previously used by Reber and co-workers to obtain a structurally related Mn^{IV} complex that exhibited weak LMCT luminescence in the solid state.^[46] A variant of this borate ligand was employed earlier by Fehlhammer and co-workers for a homoleptic Fe^{III} complex,^[47] but luminescence properties were not explored at that time (and likely would not be spectacular due to the presence of a hydrogen atom at boron instead of a phenyl-ring like in phtmeimb). The anionic nature of this scorpionate ligand, combined with the near-perfect octahedral NHC coordination of Fe^{III} , induces a particularly strong ligand field, in which the metal center has a low-spin d^5 -electron configuration, analogous to that of $[\text{Fe}(\text{btz})_3]^{3+}$. However, the ligand field in $[\text{Fe}(\text{phtmeimb})_2]^+$ is so strong that the ${}^4\text{MC}$ and ${}^6\text{MC}$ states are further destabilized by 13 and 23% relative to $[\text{Fe}(\text{btz})_3]^{3+}$, according to DFT calculations; thus causing a further increase of the activation barrier for the decay of the emissive ${}^2\text{LMCT}$ state via the ${}^4\text{MC}$ state. An Arrhenius-type analysis of temperature-dependent luminescence lifetimes yields an activation barrier of 3 kJ mol^{-1} and a pre-exponential factor of $1 \times 10^9 \text{ s}^{-1}$. For $[\text{Fe}(\text{btz})_3]^{3+}$, larger pre-exponential factors of 2×10^{10} and $2 \times 10^{13} \text{ s}^{-1}$ were found,^[41] and therefore, the longer ${}^2\text{LMCT}$ lifetime of $[\text{Fe}(\text{phtmeimb})_2]^+$ (2 ns compared with 0.1 ns) was tentatively attributed to a reduced crossing frequency from the ${}^2\text{LMCT}$ state to the ${}^4\text{MC}$ state.^[45]

${}^2\text{LMCT}$ -excited $[\text{Fe}(\text{phtmeimb})_2]^+$ is both a strong reductant ($E_{\text{ox}} = -1.9 \text{ V}$ vs. $\text{Fc}^{+/0}$) and a good oxidant ($E_{\text{red}} = 1.0 \text{ V}$ vs. $\text{Fc}^{+/0}$). Accordingly, oxidative excited-state quenching with methyl viologen and reductive quenching by diphenylamine both occur with essentially diffusion-limited kinetics.^[45] In long-term photoirradiation experiments (156 h with an 11 W fluorescent lamp), the $[\text{Fe}(\text{phtmeimb})_2]^+$ complex is remarkably robust, particularly in direct comparison to $[\text{Ru}(\text{bpy})_3]^{2+}$. The combination of respectable luminescence quantum yield, nanosecond lifetime, pronounced photoredox properties, and photostability make this complex a very interesting alternative to Ru^{II} polypyridines.

Isoelectronic Alternatives to Fe^{II} as ${}^3\text{MLCT}$ Emitters: Cr^0 and Mo^0

There are now two Fe^{III} complexes with a photoactive ${}^2\text{LMCT}$ state that are promising for hole injection into p-type semicon-

ductor photocathodes.^[41,45] However, there are still no reports on ${}^3\text{MLCT}$ luminescence from an Fe^{II} complex, and long-lived MLCT states are desirable for electron injection into n-type semiconductor photoanodes.^[23b,25b] Although the 528 ps ${}^3\text{MLCT}$ lifetime of $[\text{Fe}(\text{btz})_3]^{2+}$ seems promising and could be useful for tandem cells operating with the $[\text{Fe}(\text{btz})_3]^{2+}/[\text{Fe}(\text{btz})_3]^{3+}$ redox couple, it seems useful to consider alternatives to Fe^{II} with the d^6 valence electron configuration, in particular, $3d^6$ and $4d^6$.^[50]

Recently, we synthesized and explored a Cr^0 complex with chelating diisocyanide ligands (Figure 10a), which had a low-spin $3d^6$ -electron configuration due to the strong ligand field provided by the isocyanides.^[48] This complex luminesces

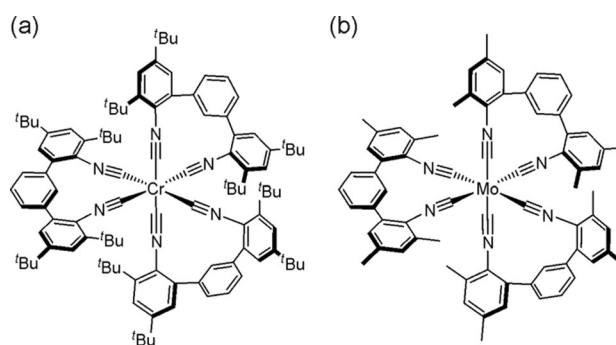


Figure 10. a) A Cr^0 complex with low-spin $3d^6$ -electron configuration (isoelectronic to $[\text{Fe}(\text{bpy})_3]^{2+}$) that exhibits ${}^3\text{MLCT}$ luminescence.^[48] b) A Mo^0 complex with low-spin $4d^6$ -electron configuration (isoelectronic to $[\text{Ru}(\text{bpy})_3]^{2+}$) that exhibits ${}^3\text{MLCT}$ luminescence.^[49]

($\lambda_{\text{max}} = 630 \text{ nm}$) from a ${}^3\text{MLCT}$ state with a quantum yield of 10^{-5} and a lifetime of 2.2 ns in deaerated THF at room temperature. To the best of our knowledge, this is the first $3d^6$ complex that exhibits MLCT luminescence in solution at room temperature,^[51] and its properties can likely be further enhanced through improved ligand design. The complex from Figure 10a was used for sensitized triplet–triplet annihilation upconversion with anthracene; thus demonstrating that bimolecular reactions are possible with its ${}^3\text{MLCT}$ state.^[52]

A Mo^0 complex with similar diisocyanide chelate ligands (Figure 10b) exhibits far better properties than its Cr^0 analogue,^[49] presumably because the $4d^6$ Mo^0 species experiences a substantially stronger ligand field than that of the $3d^6$ Cr^0 species in a similar coordination environment. ${}^3\text{MLCT}$ luminescence from the Mo^0 complex occurs with a quantum yield of 0.045 and a lifetime of 225 ns in deaerated benzene. In this long-lived excited state, its oxidation potential is -2.5 V versus $\text{Fc}^{+/0}$, which makes it a more potent photoreductant than the widely used *fac*- $[\text{Ir}(\text{ppy})_3]$ ($\text{ppy} = 2\text{-phenylpyridine}$) complex,^[42] and this was exploited for thermodynamically challenging photoredox catalysis.^[49] These Cr^0 and Mo^0 studies with chelating diisocyanides were inspired by previous work on W^0 by the group of Gray with monodentate isocyanides.^[52–53] The natural abundance of Cr and Mo is significantly lower than that of Fe, yet Cr is twice as abundant in the earth's crust than the frequently considered Cu (0.01 vs. 0.005 mass percent).^[54]

DFT studies by Uhlig and co-workers indicated that Co^{III} carbene complexes had interesting electronic structures,^[43] and recent work by Zysman-Colman and co-workers identified two emissive Co^{III} complexes that were also used for photoredox catalysis.^[55] However, these are LMCT emitters, that is, the direction of charge transfer is the same as that in the Fe^{III} complexes discussed above. Similarly, the Zr^{IV} luminophores and photocatalysts reported recently by Milsman and co-workers operated on the basis of LMCT excitations.^[56]

Summary and Outlook

The seven different concepts used to structure this survey of recent progress on photoactive iron complexes can be condensed into two overarching strategies that will likely continue to be of universal importance: 1) the use of chelating ligands that permit robust metal coordination in high symmetry, as closely to the ideal octahedral coordination as possible, to maximize the overlap between metal and ligand orbitals; and 2) the use of ligands that combine strong σ -donor and π -acceptor properties to create strong ligand fields, in which non-radiatively deactivating MC states are shifted to high energies and displaced strongly along relevant normal coordinates. Both of these strategies directly emerge from ligand field theory and as such are not novel, but many of the recent studies discussed above reported on very effective ways to implement these strategies, and some rather clear ligand design principles have now been elaborated, both experimentally and computationally.

It seems fair to state that the very recent discovery of LMCT-emissive Fe^{III} complexes came as a big surprise for many active researchers of the inorganic photophysics community, and this could be considered a disruptive change, to use a term from economy. Iron(III) complexes are likely to attract much attention from this community in the near future, considering that the necessary ligand design principles have now become so evident. The recently reported Fe^{III} complex with an anionic scorpionate tris(NHC) ligand exhibits photophysical and photochemical properties that, in several regards, come very close to those of the prototype [Ru(bpy)₃]²⁺ complex, and in terms of photorobustness seem to be even better.^[45] It remains to be seen whether the electronic structures of photoactive Fe^{III} complexes will be as widely and as readily tunable as those as Ru^{II} polypyridines. Heteroleptic Fe^{III} complexes could be interesting targets for separate tuning of HOMO and LUMO energies,^[12] similar to what is possible in cyclometalated Ir^{III} complexes.^[57]

The idea of targeting spin-allowed LMCT rather than spin-forbidden MLCT emission is fundamentally interesting and has perhaps received too little attention until now. Whether or not a spin change is involved will clearly greatly affect radiative relaxation rates and competition between luminescence and nonradiative deactivation. For the classic LMCT target cases, such as the d⁰ (e.g., Zr^{IV}^[56]) or low-spin d⁶-electron configurations (e.g., Co^{III}^[55]), spin-forbidden emission is found; hence the low-spin d⁵ configuration is special in that regard, but there are other electron configurations for which similar behavior could be expected.

Regardless of the spin issue, further consideration of LMCT and less focus on MLCT excited states could be a possible future development as well. In particular, organic photoredox catalysis has largely relied on MLCT excited states with metal-based sensitizers until now, but there are very promising avenues involving LMCT excited states.^[58] Reversal of the charge-transfer direction from MLCT to LMCT leads to sensitizers that will be better suited for hole injection into p-type semiconductors than that for electron injection into n-type semiconductors. To date, there have been no reports on an MLCT emitter based on Fe^{II}, but an isoelectronic Cr⁰ complex was recently found to be luminescent with a ³MLCT lifetime of 2.2 ns in solution at room temperature.^[48] Research along these lines, considering other earth-abundant metal elements with the 3d⁶ (or 4d⁶)^[49] electron configuration could be an interesting avenue.^[59] Exciting times are ahead in the photophysics and photochemistry of transition-metal complexes,^[60] and in some years from now we will more clearly see whether iron can indeed become the new ruthenium in these areas. A big leap forward in that direction has been made very recently.

Acknowledgements

The author thanks his co-workers for their contributions to the research performed by his group cited in this article. Their names appear in the references. Support from the Swiss National Science Foundation, currently through grant number 200021_178760 and the NCCR Molecular Systems Engineering, is gratefully acknowledged.

Conflict of interest

The author declares no conflict of interest.

Keywords: iron • ligand design • luminescence • photophysics • sustainable chemistry

- [1] A. Juris, V. Balzani, F. Barigelletti, S. Campagna, P. Belser, A. Von Zelewsky, *Coord. Chem. Rev.* **1988**, *84*, 85–277.
- [2] N. H. Damrauer, G. Cerullo, A. Yeh, T. R. Bousie, C. V. Shank, J. K. McCusker, *Science* **1997**, *275*, 54–57.
- [3] Q. C. Sun, S. Mosquera-Vazquez, Y. Suffren, J. Hankache, N. Amstutz, L. M. L. Daku, E. Vauthey, A. Hauser, *Coord. Chem. Rev.* **2015**, *282*, 87–99.
- [4] Q. C. Sun, B. Dereka, E. Vauthey, L. M. L. Daku, A. Hauser, *Chem. Sci.* **2017**, *8*, 223–230.
- [5] E. A. Medlycott, G. S. Hanan, *Chem. Soc. Rev.* **2005**, *34*, 133–142.
- [6] E. A. Juban, A. L. Smeigh, J. E. Monat, J. K. McCusker, *Coord. Chem. Rev.* **2006**, *250*, 1783–1791.
- [7] a) A. Cannizzo, C. J. Milne, C. Consani, W. Gawelda, C. Bressler, F. van Mourik, M. Chergui, *Coord. Chem. Rev.* **2010**, *254*, 2677–2686; b) W. K. Zhang, K. J. Gaffney, *Acc. Chem. Res.* **2015**, *48*, 1140–1148; c) G. Auböck, M. Chergui, *Nat. Chem.* **2015**, *7*, 629–633.
- [8] a) A. Gualandi, M. Marchini, L. Mengozzi, M. Natali, M. Lucarini, P. Ceroni, P. G. Cozzi, *ACS Catal.* **2015**, *5*, 5927–5931; b) S. Parisien-Collette, A. C. Hernandez-Perez, S. K. Collins, *Org. Lett.* **2016**, *18*, 4994–4997; c) C. B. Larsen, O. S. Wenger, *Chem. Eur. J.* **2018**, *24*, 2039–2058.
- [9] J. V. Caspar, T. J. Meyer, *J. Phys. Chem.* **1983**, *87*, 952–957.
- [10] M. C. Carey, S. L. Adelman, J. K. McCusker, *Chem. Sci.* **2019**, *10*, 134–144.
- [11] L. L. Jamula, A. M. Brown, D. Guo, J. K. McCusker, *Inorg. Chem.* **2014**, *53*, 15–17.

- [12] A. K. C. Mengel, C. Förster, A. Breivogel, K. Mack, J. R. Ochsmann, F. Laquai, V. Ksenofontov, K. Heinze, *Chem. Eur. J.* **2015**, *21*, 704–714.
- [13] a) S. M. Fatur, S. G. Shepard, R. F. Higgins, M. P. Shores, N. H. Damrauer, *J. Am. Chem. Soc.* **2017**, *139*, 4493–4505; b) S. G. Shepard, S. M. Fatur, A. K. Rappe, N. H. Damrauer, *J. Am. Chem. Soc.* **2016**, *138*, 2949–2952.
- [14] Y. Z. Liu, T. Harlang, S. E. Canton, P. Chabera, K. Suarez-Alcantara, A. Fleckhaus, D. A. Vithanage, E. Goransson, A. Corani, R. Lomoth, V. Sundström, K. Wärnmark, *Chem. Commun.* **2013**, *49*, 6412–6414.
- [15] D. Leshchev, T. C. B. Harlang, L. A. Fredin, D. Khakhulin, Y. Z. Liu, E. Biasin, M. G. Laursen, G. E. Newby, K. Haldrup, M. M. Nielsen, K. Wärnmark, V. Sundström, P. Persson, K. S. Kjaer, M. Wulff, *Chem. Sci.* **2018**, *9*, 405–414.
- [16] P. Zimmer, L. Burkhardt, A. Friedrich, J. Steube, A. Neuba, R. Schepper, P. Müller, U. Florke, M. Huber, S. Lochbrunner, M. Bauer, *Inorg. Chem.* **2018**, *57*, 360–373.
- [17] a) S. Mukherjee, D. N. Bowman, E. Jakubikova, *Inorg. Chem.* **2015**, *54*, 560–569; b) I. M. Dixon, F. Alary, M. Boggio-Pasqua, J. L. Heully, *Dalton Trans.* **2015**, *44*, 13498–13503; c) I. M. Dixon, S. Khan, F. Alary, M. Boggio-Pasqua, J. L. Heully, *Dalton Trans.* **2014**, *43*, 15898–15905.
- [18] P. Chábera, K. S. Kjaer, O. Prakash, A. Honarfar, Y. Z. Liu, L. A. Fredin, T. C. B. Harlang, S. Lidin, J. Uhlig, V. Sundström, R. Lomoth, P. Persson, K. Wärnmark, *J. Phys. Chem. Lett.* **2018**, *9*, 459–463.
- [19] D. N. Bowman, A. Bondarev, S. Mukherjee, E. Jakubikova, *Inorg. Chem.* **2015**, *54*, 8786–8793.
- [20] C. Förster, M. Dorn, T. Reuter, S. Otto, G. Davarci, T. Reich, L. Carrella, E. Rentschler, K. Heinze, *Inorganics* **2018**, *6*, 86.
- [21] A. K. C. Mengel, C. Bissinger, M. Dorn, O. Back, C. Förster, K. Heinze, *Chem. Eur. J.* **2017**, *23*, 7920–7931.
- [22] A. Cannizzo, A. M. Blanco-Rodriguez, A. El Nahhas, J. Šebera, S. Zális, A. Vlček, M. Chergui, *J. Am. Chem. Soc.* **2008**, *130*, 8967–8974.
- [23] a) Y. Z. Liu, P. Persson, V. Sundström, K. Wärnmark, *Acc. Chem. Res.* **2016**, *49*, 1477–1485; b) T. Duchanois, L. Liu, M. Pastore, A. Monari, C. Cebrian, Y. Trolez, M. Darari, K. Magra, A. Frances-Monerris, E. Domenichini, M. Beley, X. Assfeld, S. Haacke, P. C. Gros, *Inorganics* **2018**, *6*, 63.
- [24] L. Liu, T. Duchanois, T. Etienne, A. Monari, M. Beley, X. Assfeld, S. Haacke, P. C. Gros, *Phys. Chem. Chem. Phys.* **2016**, *18*, 12550–12556.
- [25] a) T. Duchanois, T. Etienne, C. Cebrian, L. Liu, A. Monari, M. Beley, X. Assfeld, S. Haacke, P. C. Gros, *Eur. J. Inorg. Chem.* **2015**, 2469–2477; b) T. C. B. Harlang, Y. Z. Liu, O. Gordivska, L. A. Fredin, C. S. Fonseca, P. Huang, P. Chabera, K. S. Kjaer, H. Mateos, J. Uhlig, R. Lomoth, R. Wallenberg, S. Styring, P. Persson, V. Sundström, K. Wärnmark, *Nat. Chem.* **2015**, *7*, 883–889.
- [26] M. Pastore, T. Duchanois, L. Liu, A. Monari, X. Assfeld, S. Haacke, P. C. Gros, *Phys. Chem. Chem. Phys.* **2016**, *18*, 28069–28081.
- [27] L. A. Fredin, K. Wärnmark, V. Sundström, P. Persson, *ChemSusChem* **2016**, *9*, 667–675.
- [28] E. Jakubikova, D. N. Bowman, *Acc. Chem. Res.* **2015**, *48*, 1441–1449.
- [29] T. Duchanois, T. Etienne, M. Beley, X. Assfeld, E. A. Perpete, A. Monari, P. C. Gros, *Eur. J. Inorg. Chem.* **2014**, 3747–3753.
- [30] P. Zimmer, P. Müller, L. Burkhardt, R. Schepper, A. Neuba, J. Steube, F. Dietrich, U. Flörke, S. Mangold, M. Gerhards, M. Bauer, *Eur. J. Inorg. Chem.* **2017**, 1504–1509.
- [31] L. A. Fredin, M. Papai, E. Rozsalyi, G. Vanko, K. Wärnmark, V. Sundström, P. Persson, *J. Phys. Chem. Lett.* **2014**, *5*, 2066–2071.
- [32] A. Francés-Monerris, K. Magra, M. Darari, C. Cebrian, M. Beley, E. Domenichini, S. Haacke, M. Pastore, X. Assfeld, P. C. Gros, A. Monari, *Inorg. Chem.* **2018**, *57*, 10431–10441.
- [33] I. M. Dixon, F. Alary, M. Boggio-Pasqua, J. L. Heully, *Inorg. Chem.* **2013**, *52*, 13369–13374.
- [34] a) C. Kreitner, K. Heinze, *Dalton Trans.* **2016**, *45*, 13631–13647; b) C. Kreitner, E. Erdmann, W. W. Seidel, K. Heinze, *Inorg. Chem.* **2015**, *54*, 11088–11104.
- [35] S. Mukherjee, D. E. Torres, E. Jakubikova, *Chem. Sci.* **2017**, *8*, 8115–8126.
- [36] D. C. Ashley, S. Mukherjee, E. Jakubikova, *Dalton Trans.* **2019**, *48*, 374–378.
- [37] I. M. Dixon, G. Boissard, H. Whyte, F. Alary, J. L. Heully, *Inorg. Chem.* **2016**, *55*, 5089–5091.
- [38] M. Wächtler, J. Kübel, K. Barthelmes, A. Winter, A. Schmiedel, T. Pascher, C. Lambert, U. S. Schubert, B. Dietzek, *Phys. Chem. Chem. Phys.* **2016**, *18*, 2350–2360.
- [39] Y. Z. Liu, K. S. Kjaer, L. A. Fredin, P. Chabera, T. Harlang, S. E. Canton, S. Lidin, J. X. Zhang, R. Lomoth, K. E. Bergquist, P. Persson, K. Wärnmark, V. Sundström, *Chem. Eur. J.* **2015**, *21*, 3628–3639.
- [40] S. Hohloch, L. Suntrup, B. Sarkar, *Organometallics* **2013**, *32*, 7376–7385.
- [41] P. Chábera, Y. Liu, O. Prakash, E. Thyrhaug, A. El Nahhas, A. Honarfar, S. Essén, L. A. Fredin, T. C. B. Harlang, K. S. Kjaer, K. Handrup, F. Ericsson, Y. Tatsuno, K. Morgan, J. Schnadt, L. Häggström, T. Ericsson, A. Sobkowiak, S. Lidin, P. Huang, S. Styring, J. Uhlig, J. Bendix, R. Lomoth, V. Sundström, P. Persson, K. Wärnmark, *Nature* **2017**, *543*, 695–699.
- [42] D. M. Arias-Rotondo, J. K. McCusker, *Chem. Soc. Rev.* **2016**, *45*, 5803–5820.
- [43] F. Ericson, A. Honarfar, O. Prakash, H. Tatsuno, L. A. Fredin, K. Handrup, P. Chabera, O. Gordivska, K. S. Kjaer, Y. Z. Liu, J. Schnadt, K. Wärnmark, V. Sundström, P. Persson, J. Uhlig, *Chem. Phys. Lett.* **2017**, *683*, 559–566.
- [44] B. Sarkar, L. Suntrup, *Angew. Chem. Int. Ed.* **2017**, *56*, 8938–8940; *Angew. Chem.* **2017**, *129*, 9064–9066.
- [45] K. S. Kjaer, N. Kaul, O. Prakash, P. Chábera, N. W. Rosemann, A. Honarfar, O. Gordivska, L. A. Fredin, K. E. Bergquist, L. Häggström, T. Ericsson, L. Lindh, A. Yartsev, S. Styring, P. Huang, J. Uhlig, J. Bendix, D. Strand, V. Sundström, P. Persson, R. Lomoth, W. Wärnmark, *Science* **2018**, *363*, 249–253.
- [46] V. Baslon, J. P. Harris, C. Reber, H. E. Colmer, T. A. Jackson, A. P. Forshaw, J. M. Smith, R. A. Kinney, J. Telsler, *Can. J. Chem.* **2017**, *95*, 547–552.
- [47] U. Kernbach, M. Ramm, P. Luger, W. P. Fehlhammer, *Angew. Chem. Int. Ed. Engl.* **1996**, *35*, 310–312; *Angew. Chem.* **1996**, *108*, 333–335.
- [48] L. A. Büldt, X. Guo, R. Vogel, A. Prescimone, O. S. Wenger, *J. Am. Chem. Soc.* **2017**, *139*, 985–992.
- [49] L. A. Büldt, X. Guo, A. Prescimone, O. S. Wenger, *Angew. Chem. Int. Ed.* **2016**, *55*, 11247–11250; *Angew. Chem.* **2016**, *128*, 11413–11417.
- [50] O. S. Wenger, *J. Am. Chem. Soc.* **2018**, *140*, 13522–13533.
- [51] a) L. A. Büldt, O. S. Wenger, *Chem. Sci.* **2017**, *8*, 7359–7367; b) L. A. Büldt, O. S. Wenger, *Dalton Trans.* **2017**, *46*, 15175–15177.
- [52] L. A. Büldt, O. S. Wenger, *Angew. Chem. Int. Ed.* **2017**, *56*, 5676–5682; *Angew. Chem.* **2017**, *129*, 5770–5776.
- [53] a) K. R. Mann, H. B. Gray, G. S. Hammond, *J. Am. Chem. Soc.* **1977**, *99*, 306–307; b) W. Sattler, L. M. Henling, J. R. Winkler, H. B. Gray, *J. Am. Chem. Soc.* **2015**, *137*, 1198–1205.
- [54] A. F. Holleman, N. Wiberg, *Lehrbuch der Anorganischen Chemie*, 102th ed., Walter de Gruyter, Berlin, **2007**.
- [55] A. K. Pal, C. F. Li, G. S. Hanan, E. Zysman-Colman, *Angew. Chem. Int. Ed.* **2018**, *57*, 8027–8031; *Angew. Chem.* **2018**, *130*, 8159–8163.
- [56] Y. Zhang, T. S. Lee, J. L. Petersen, C. Milsman, *J. Am. Chem. Soc.* **2018**, *140*, 5934–5947.
- [57] M. S. Lowry, S. Bernhard, *Chem. Eur. J.* **2006**, *12*, 7970–7977.
- [58] Y. Qiao, E. J. Schelter, *Acc. Chem. Res.* **2018**, *51*, 2926–2936.
- [59] J. K. McCusker, *Science* **2019**, *363*, 484–488.
- [60] E. R. Young, A. Oldacre, *Science* **2019**, *363*, 225–226.

Manuscript received: December 11, 2018
 Revised manuscript received: January 3, 2019
 Accepted manuscript online: January 7, 2019
 Version of record online: February 18, 2019